AN APPLICATION OF THE HYBRID DIFFERENTIAL TRANSFORM-FINITE DIFFERENCE METHOD FOR STUDYING A THIN FILM EXPOSED TO ULTRASHORT-PULSED LASERS

Lo C.Y.
Department of Aeronautical Engineering
National Formosa University
Huwei, Yunlin 632
Taiwan
E-mail: cylo@nfu.edu.tw

ABSTRACT

The present work presents a numerical approach using the hybrid differential transform/finite difference method to study heat transfer in a thin film exposed to ultrashort-pulsed lasers. This problem involving high energy flux caused by lasers within a very short duration is formulated based on the hyperbolic two-step model that includes the features of finite speed of thermal wave and the coupling effects of energy flux between the electron-lattice systems. The governing equations are transformed from the time domain into the spectrum domain using the differential transform technique. The numerical solutions are obtained through a recursive process associated with the discretized equations in the space domain using the finite difference method. An axisymmetric case of a gold film subjected to a laser beam is given as a numerical example. Both the electron and lattice temperatures are obtained by the proposed method.

INTRODUCTION

Laser manufacturing technique has been playing a very important role in the modern precision manufacturing. Some materials with properties such as high thermal conductivities or low melting point are difficult to fabricate because laser energy could diffuse in the materials that greatly reduce precision and quality of laser manufacturing. Reducing the duration of laser pulses can help alleviate energy dissipation. Because the ability to improve precision and reduce thermal damage with very short pulse duration, ranging from sub-picosecond to femtoseconds, ultrashort-pulsed lasers have increasing applications in a variety of fields such as engineering, science and medicine [1-3]. The applications of ultrashort-pulse lasers involve the high rate of energy exchange within an extremely short period of time in which thermal equilibrium can not be established immediately because the electron system has much smaller heat capacity than the lattice system. Anisimov [4] proposed a two-step model to account for the highly unstable absorption process of laser energy. The process is divided into two steps. First, the laser energy is absorbed by electrons and the electron temperature increases. Then, electron energy flows into the lattice system through the coupling effects of heat transfer between the electron and the lattice.

NOMENCLATURE		
C	[J/m³K]	Heat capacity
G	[W/m³K]	Electron-lattice coupling factor
J	[J/m²]	Laser fluence
k	[W/mK]	Thermal conductivity
L	[μm]	Length
q_i	[W/m²]	Heat flux
Q	[-]	Differential transform of heat flux q
t	[ps]	Time
t_p	[ps]	Laser pulse duration
T	[K]	Temperature
$\widetilde{T}$	[-]	Differential Transform of temperature T
r_s	[μm]	Spatial profile parameter of laser
r	[μm]	Cylindrical axis coordinate
S	[W/m³]	Laser energy absorption rate
$\widetilde{S}$	[-]	Differential Transform of Laser energy absorption rate S
z	[μm]	Cylindrical axis coordinate
z_s	[μm]	Optical penetration depth
τ	[ps]	Relaxation time
Subscripts and Superscripts		
r	[-]	Cylindrical axis direction
z	[-]	Cylindrical axis direction
e	[-]	Electron
l	[-]	Lattice
i,j,k	[-]	Integer index

The pulse duration of ultrashort-pulsed lasers lasts a very short period. The highly unstable heat flux causes significant temperature gradient in the materials. Under the circumstances, the Fourier heat transfer model is not appropriate because the effects of the speed of thermal wave are no longer able to be neglected. The hyperbolic heat transfer model is much suitable for this kind of problems. Tien and Qiu [5,6] provided the fundamental basis for the applications of the hyperbolic two-step model to laser manufacturing by calculating macroscopic physical quantities of electric and heat flux. Several researchers [7-10] studied heat transfer in a thin film exposed to ultrashort-pulsed lasers based on the hyperbolic two-step model. The success in determining physical properties, including the

electron heat capacity, electron relaxation time, electron conductivity, reflectivity, and absorption coefficient using full-run quantum treatments by Jiang and Tsai [11] makes the applications of the hyperbolic two-step model more feasible and practical.

Hyperbolic heat transfer problems have been widely studied using a variety of methods [12-14]. Differential transformation method [15,16] is a function transformation technique based on Taylor's series. The present paper applies the hybrid differential transform/finite difference method to solve the problems of heat transfer in a thin film subjected to an ultrashort-pulsed laser. An axisymmetric case of a gold film subjected to a laser beam is given as a numerical example.

MATHEMATICAL MODEL

Consider a 2-D axisymmetric thin film exposed to an ultrashort-pulsed laser acting at the origin as shown in Figure 1. The thin film made of gold has a diameter of 5μm and a thickness of 0.1μm. The laser energy absorbed by electrons is represented as the Gaussian heat source function [7-10]

$$S = 0.94J \frac{1-R}{t_p z_s} \exp[-\frac{z}{z_s} - \frac{r^2}{r_s^2} - 2.77(\frac{t-2t_p}{t_p})^2] \quad (1)$$

where S is the energy absorption rate, J is laser fluence, R is surface reflectivity, t_p is laser pulse duration, z_s is optical penetration depth and r_s is spatial profile parameter. The material properties of gold are listed in Table 1.
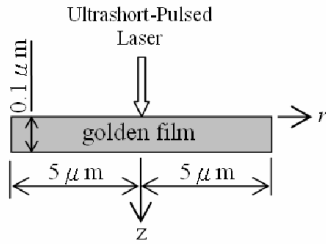

Figure 1 A 2-D axisymmetric thin film irradiated by a laser

Based on the hyperbolic two-step model, the laser energy is first absorbed by electrons and then transfer from the electron system to the lattice system. The governing equations can be given as follow [17]

Electron energy equations

$$C_e(T_e)\frac{\partial T_e}{\partial t} = -\frac{q_e^r}{r} - \frac{\partial q_e^r}{\partial r} - \frac{\partial q_e^z}{\partial z} - G(T_e - T_l) + S \quad (2)$$

$$\tau_e \frac{\partial q_e^r}{\partial t} + q_e^r = -k_e \frac{\partial T_e}{\partial r} \quad (3)$$

$$\tau_e \frac{\partial q_e^z}{\partial t} + q_e^z = -k_e \frac{\partial T_e}{\partial z} \quad (4)$$

Lattice energy equations

$$C_l \frac{\partial T_l}{\partial t} = -\frac{q_l^r}{r} - \frac{\partial q_l^r}{\partial r} - \frac{\partial q_l^z}{\partial z} + G(T_e - T_l) \quad (5)$$

$$\tau_l \frac{\partial q_l^r}{\partial t} + q_l^r = -k_l \frac{\partial T_l}{\partial r} \quad (6)$$

$$\tau_l \frac{\partial q_l^z}{\partial t} + q_l^z = -k_l \frac{\partial T_l}{\partial z} \quad (7)$$

where T_e is electron temperature, T_l is lattice temperature, T_o is initial temperature, electron heat capacity $C_e(T_e)=C_{e0}(T_e/T_l)$ and electron thermal conductivity $k_e(T_e,T_l)=k_0(T_e/T_l)$ are given as function of the electron and lattice temperature, k_l is lattice thermal conductivity, G is electron-lattice coupling factor, C_l is lattice heat capacity, τ_e and τ_l are electron and lattice relaxation time. q_e^r, q_e^z are the electron heat flux in r and z axes, and q_l^r, q_l^z are the lattice heat flux in r and z axes, respectively.

Eq. (2)-(4) and Eq. (5)-(7) represent energy conservation in the electron system and in the lattice system, respectively. The coupling effects of heat transfer between the electron and lattice systems are given in Eq. (2) and (4). The effects of time lag in heat transfer are given in Eq. (3), (4) and Eq. (6), (7). The model is reduced to the conventional parabolic heat transfer model if both τ_e and τ_l vanish. If the electron temperature and the lattice temperature are kept the same ($T_e=T_l$), the model is further reduced to the one-step model.

The uniformly distributed electron and lattice temperature are set to be $T_0=300^\circ K$ and no heat flux exists at the beginning.

Initial conditions:

$$\begin{aligned} T_e = T_l = T_0 = 300 \\ q_e^r = q_e^z = q_l^r = q_l^z = 0 \end{aligned} \quad at \quad t = 0 \quad (8)$$

Heat flux across the surface of the thin film is neglected.

Boundary conditions:

$$\begin{aligned} q_e^z = q_l^z = 0 \qquad at \qquad r = 0, r = 5 \\ q_e^r = q_l^r = 0 \qquad at \qquad z = 0, z = 0.1 \end{aligned} \quad (9)$$

Table 1. Material properties of gold

C_{e0}	$2.1 \times 10^{-14} J/\mu m^3 K$	R	0.93
C_l	$2.5 \times 10^{-12} J/\mu m^3 K$	r_s	$1\mu m$
G	$2.6 \times 10^{10} J/\mu m^3 K$	y_s	$1.52 \times 10^{-3} \mu m$
J	$500 \times 10^{-12} J/\mu m^2$	t_p	$0.1 ps$
k_0	$315 \times 10^{-6} W/\mu m^2 K$	τ_e	$0.04 ps$
k_l	$315 \times 10^{-6} W/\mu m^2 K$	τ_l	$0.8 ps$

DIFFERENTIAL TRANSFORM AND NUMERICAL METHOD

The differential transform is one of transformation technique based on Taylor's expansion series. Assuming that $f(t)$ is an analytic function in the time domain, the differential transform of $f(t)$ at $t=0$ is defined by

$$F(k) = T[f(t)] = \frac{H^k}{k!} \left[\frac{d^k f(t)}{dt^k} \right]_{t=0} \quad k = 1, 2, 3, \cdots \quad (10)$$

where H is the time span of differential transformation. $F(k)$ is called the spectrum of $f(t)$ in the spectrum domain. The original analytic function $f(t)$ can be given by the inverse differential transform as the infinite sum in Eq. (11). In practice, $f(t)$ is usually approximated by the n-th partial sum of power series

$$f(t) = \sum_{k=0}^{\infty}\left(\frac{t}{H}\right)^k F(k) \quad \text{or} \quad f(t) = \sum_{k=0}^{n}\left(\frac{t}{H}\right)^k F(k) \tag{11}$$

The addition and multiplication are defined directly based on the operation of Taylor's series. Assume that $h(t)=f(t)g(t)$, $z(t)=f(t)/g(t)$ and $T[f(t)]=F(k)$, $T[g(t)]=G(k)$, then the differential transform of $h(t)$ and $z(t)$ are defined as follow

$$H(k) = T[h(t)] = \sum_{l=0}^{k} F(l)G(k-l)$$

$$Z(k) = T[z(t)] = \frac{F(k) - \sum_{l=0}^{k-1}\left[F(l)\Big/G(l)\right]G(k-l)}{G(0)} \tag{12}$$

The following numerical procedures for applying the hybrid differential transform / finite difference method are used to solve the current 2-D axisymmetric heat transfer problem of a thin film exposed to an ultrashort-pulsed laser. First, apply the differential transformation technique to the governing equations, Eq. (1)~(7), with respect to the time t. The resulting transform equations in a recursive form are

Recursive electron energy equations:

$$\frac{C_{e0}}{T_0}\left[\tilde{T}_e(0)\cdot\frac{k+1}{H}\cdot\tilde{T}_e(k+1)\right] =$$
$$-\frac{Q_e^r(k)}{r} - \frac{\partial Q_e^r(k)}{\partial r} - \frac{\partial Q_e^z(k)}{\partial z} - G[\tilde{T}_e(k) - \tilde{T}_l(k)] + \tilde{S}(k)$$
$$-\frac{C_{e0}}{T_0}\left[\sum_{l=1}^{k}\tilde{T}_e(l)\cdot\frac{k-l+1}{H}\cdot\tilde{T}_e(k-l+1)\right]$$
$$\dots\dots\dots\dots\dots\dots\dots\dots\dots\dots\dots\dots\dots\dots\dots\dots\dots\tag{13}$$

$$\tau_e\frac{k+1}{H}Q_e^r(k+1)$$
$$= -\frac{k_0}{T_l(0)}\left[\tilde{T}_e(k) - \sum_{l=0}^{k-1}[\tilde{T}_e(l)/\tilde{T}_l(l)]\cdot\tilde{T}_l(k-l)\right]\frac{\partial\tilde{T}_e(k)}{\partial r} - Q_e^r(k)$$
$$\dots\dots\dots\dots\dots\dots\dots\dots\dots\dots\dots\dots\dots\dots\dots\dots\dots\tag{14}$$

$$\tau_e\frac{k+1}{H}Q_e^z(k+1)$$
$$= -\frac{k_0}{T_l(0)}\left[\tilde{T}_e(k) - \sum_{l=0}^{k-1}[\tilde{T}_e(l)/\tilde{T}_l(l)]\cdot\tilde{T}_l(k-l)\right]\frac{\partial\tilde{T}_e(k)}{\partial z} - Q_e^z(k)$$
$$\dots\dots\dots\dots\dots\dots\dots\dots\dots\dots\dots\dots\dots\dots\dots\dots\dots\tag{15}$$

Recursive lattice energy equations:

$$C_l\frac{k+1}{H}\tilde{T}(k+1) =$$
$$-\frac{Q_l^r(k)}{r} - \frac{\partial Q_l^r(k)}{\partial r} - \frac{\partial Q_l^z(k)}{\partial z} + G[\tilde{T}_e(k) - \tilde{T}_l(k)] \quad\dots\dots\dots\dots\tag{16}$$

$$\tau_l\frac{k+1}{H}Q_l^r(k+1) = -k_l\frac{\partial\tilde{T}_l(k)}{\partial r} - Q_l^r(k) \dots\dots\dots\dots\dots\dots\dots\tag{17}$$

$$\tau_l\frac{k+1}{H}Q_l^z(k+1) = -k_l\frac{\partial\tilde{T}_l(k)}{\partial z} - Q_l^z(k) \dots\dots\dots\dots\dots\dots\dots\tag{18}$$

where the capital letters represent the differential transforms of the functions of the corresponding lowercase letters, i.e., Q_l^x is the transform function of q_l^x. Also, $\tilde{T}_e(k), \tilde{T}_l(k), \tilde{S}(k)$ are the transform functions of $T_e(t)$, $T_l(t)$, $S(t)$, respectively. Eq. (13)-

(18) are recursive equations, which means the k-th order values can be calculated from the previous $(k$-$1)$-th order results. Because of symmetry, the right-half space domain is divided equally into $n_r \times n_z$ equal subintervals, r_i, $i=1,2,3\dots,n_r+1$ and z_j, $j=1,2,3,\dots,n_z+1$. The above equations are further discretized by the finite difference method on each node as

Discretized electron energy equations:

$$\frac{C_{e0}}{T_0}\left[(\tilde{T}_e)_{i,j}(0)\cdot\frac{k+1}{H}\cdot(\tilde{T}_e)_{i,j}(k+1)\right] =$$
$$-\frac{(Q_e^r)_i}{r_i} - \frac{1}{2dr}[(Q_e^r)_{i+1,j}(k) - (Q_e^r)_{i-1,j}(k)]$$
$$-\frac{1}{2dz}[(Q_e^z)_{i,j+1}(k) - (Q_e^z)_{i,j-1}(k)] - G[(\tilde{T}_e)_{i,j}(k) - (\tilde{T}_l)_{i,j}(k)] + \tilde{S}(k)$$
$$-\frac{C_{e0}}{T_0}\left[\sum_{l=1}^{k}(\tilde{T}_e)_{i,j}(l)\cdot\frac{k-l+1}{H}\cdot(\tilde{T}_e)_{i,j}(k-l+1)\right]$$
$$\dots\dots\dots\dots\dots\dots\dots\dots\dots\dots\dots\dots\dots\dots\dots\dots\dots\tag{19}$$

$$\tau_e\frac{k+1}{H}(Q_e^r)_{i,j}(k+1)$$
$$= -\frac{k_0}{T_l(0)}\frac{1}{2dr}\left[(\tilde{T}_e)_{i,j}(k) - \sum_{l=0}^{k-1}[(\tilde{T}_e)_{i,j}(l)/(\tilde{T}_l)_{i,j}(l)]\cdot(\tilde{T}_l)_{i,j}(k-l)\right]$$
$$\cdot[(\tilde{T}_e)_{i+1,j}(k) - (\tilde{T}_e)_{i-1,j}(k)] - (Q_e^r)_{i,j}(k)$$
$$\dots\dots\dots\dots\dots\dots\dots\dots\dots\dots\dots\dots\dots\dots\dots\dots\tag{20}$$

$$\tau_e\frac{k+1}{H}(Q_e^z)_{i,j}(k+1)$$
$$= -\frac{k_0}{T_l(0)}\frac{1}{2dz}\left[(\tilde{T}_e)_{i,j}(k) - \sum_{l=0}^{k-1}[(\tilde{T}_e)_{i,j}(l)/(\tilde{T}_l)_{i,j}(l)]\cdot(\tilde{T}_l)_{i,j}(k-l)\right]$$
$$\cdot[(\tilde{T}_e)_{i+1,j}(k) - (\tilde{T}_e)_{i-1,j}(k)] - (Q_e^z)_{i,j}(k)$$
$$\dots\dots\dots\dots\dots\dots\dots\dots\dots\dots\dots\dots\dots\dots\dots\dots\tag{21}$$

Discretized lattice energy equations:

$$C_l\frac{k+1}{H}(T_l)_{i,j}(k+1) = -\frac{(Q_l^r)_{i,j}(k)}{r_i}$$
$$-\frac{1}{2dr}[(Q_l^r)_{i+1,j}(k) - (Q_l^r)_{i-1,j}(k)] \qquad\qquad\dots\tag{22}$$
$$-\frac{1}{2dz}[(Q_l^z)_{i,j+1}(k) - (Q_l^z)_{i,j-1}(k)] + G[(\tilde{T}_e)_{i,j}(k) - (\tilde{T}_l)_{i,j}(k)]$$

$$\tau_l\frac{k+1}{H}(Q_l^r)_{i,j}(k+1)$$
$$\qquad\qquad\qquad\qquad\qquad\dots\dots\dots\dots\tag{23}$$
$$= -\frac{k_l}{2dr}[(\tilde{T}_l)_{i+1,j}(k) - (\tilde{T}_l)_{i-1,j}(k)] - (Q_l^r)_{i,j}(k)$$

$$\tau_l\frac{k+1}{H}(Q_l^z)_{i,j}(k+1)$$
$$\qquad\qquad\qquad\qquad\qquad\dots\dots\dots\dots\dots\tag{24}$$
$$= -\frac{k_l}{2dz}[(\tilde{T}_l)_{i,j+1}(k) - (\tilde{T}_l)_{i,j-1}(k)] - (Q_l^z)_{i,j}(k)$$

Boundary conditions and initial conditions given in the spectrum domain are

Initial conditions:

$$(\tilde{T}_e)_{i,j}(k) = (\tilde{T}_l)_{i,j}(k) = T_0 \text{ at } k=0 \text{ for all } i,j$$
$$(Q_l^x)_{i,j}(k) = (Q_l^y)_{i,j}(k) = 0 \text{ at } k=0 \text{ for all } i,j \dots\dots\dots\dots\tag{26}$$
$$(Q_e^x)_{i,j}(k) = (Q_e^y)_{i,j}(k) = 0 \text{ at } k=0 \text{ for all } i,j$$

Boundary conditions:

$$(Q_e^r)_{i,j} = (Q_l^r)_{i,j} = 0 \qquad \text{at } i = 1 \text{ and } n_r + 1 \text{ for all } k$$
$$(Q_l^{\bar{z}})_{i,j} = (Q_l^{\bar{z}})_{i,j} = 0 \qquad \text{at } j = 1 \text{ and } n_z + 1 \text{ for all } k \quad \cdots\cdots(27)$$

Transform function of system variables at k=0 are given in the initial conditions. The higher order values ($k \geq 1$) of the transform functions are calculated from the recursive equations and boundary conditions. The values of system variables are determined using the inverse differential transform method with the n-partial sum (Eq.11) However, the differential transform is only applicable within the time span, $0 \leq t \leq H$. When a large time span is used, it requires large n to achieve accurate convergent values. Therefore, in practical applications, in order to increase the convergence rate and to improve the accuracy of solutions, it is usual to divide the time intervals t into smaller time increments $\triangle t$. The above numerical procedure is carried out sequentially at each time increment $\triangle t$, setting H=$\triangle t$ for each time increment. The initial conditions at each time increment are obtained from the numerical solution at the previous time increment.

NUMERICAL RESULTS AND DISCUSSION

The accuracy of analysis depends on the size of the time span (time increment) and the terms of the partial sum in the inverse process. Generally speaking, a larger time span requires more terms used in the partial sum. The 7-order partial sum (n=7) is used throughout this analysis. Four different time spans, H=0.01ps, 0.0025ps, 0.0005ps, and 0.0001ps are used to check the accuracy by comparing the values of the simulated laser heat source function to the exact laser heat source function at the origin (r=0, z=0), which is the centre of the projecting laser beam. The comparison is shown in Figure 2. Laser fluence is set to be J=$500 \times 10^{-12} J/\mu m^2$.and pulse duration is set to be t_p= 0.2ps. The laser intensity reaches its maximum at t=0.2ps. There is a very small difference between the simulated source function and exact source function for H=0.0001ps. Hence, this time span is used as time increments through out the paper.
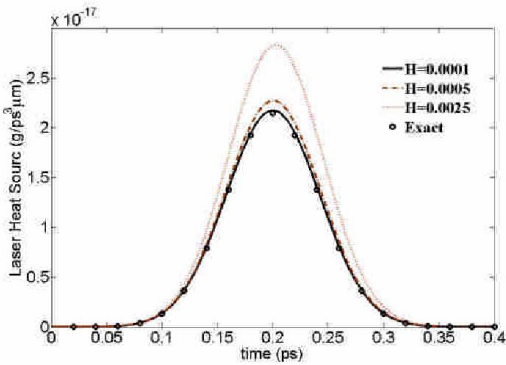

Figure 2 Comparison of simulated and exact laser heat source function at the origin (r=0,z=0)

The adequacy of mesh selection is checked by the convergence test with different mesh sizes, 20×20, 30×30, 40×40, 50×50. Figure 3 shows the electron temperature at the origin for $0ps \leq t \leq 0.5ps$. Laser fluence and pulse duration are kept unchanged. The results show that 20×20 mesh and 30×30

mesh are too coarse to obtain the accurate solution. On the other hand, the electron temperatures from 40×40 mesh and 50×50 mesh have a very good match. Hence, the 50×50 mesh is used in the remaining analysis.
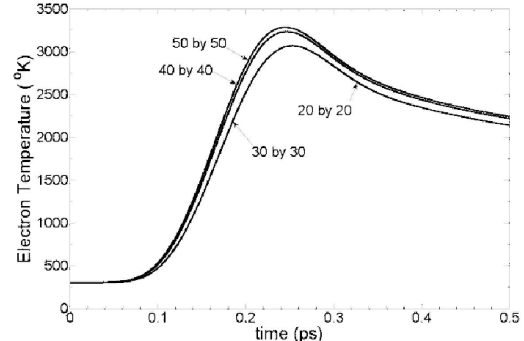

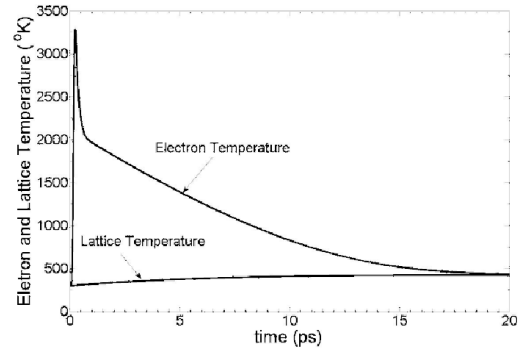**Figure 3** Electron temperature at the origin (r=0,z=0) for various mesh (20×20, 30×30, 40×40, 50×50)

Figure 4 The electron and lattice temperature at the origin (r=0, z=0) for J=$500 \times 10^{-12} J/\mu m^2$.
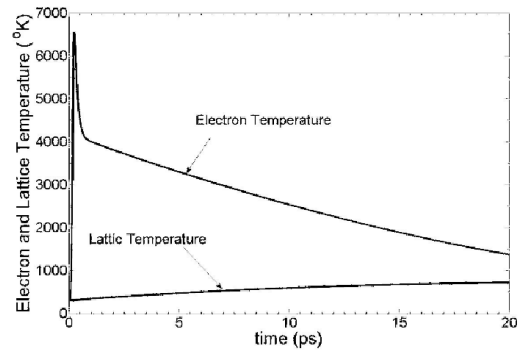

Figure 5 The electron and lattice temperature at the origin (r=0, z=0) for J=$2000 \times 10^{-12} J/\mu m^2$.

The electron and lattice temperatures at the origin for J=$500 \times 10^{-12} J/\mu m^2$. are shown in Figure 4. Because the laser energy is absorbed by free electrons first, the electron temperature rises to 3300°K rapidly when the laser pulse is applied. After the laser pulse vanishes, the electron temperature gradually reduce to about 420 °K at t=20ps. Over the same period of time, the lattice temperature gradually increases by

the energy flux from the electron system through the coupling effects. The rate of temperature change in the electron system is fast than that in the lattice system because the electron system has much smaller heat capacity than the lattice system. After the laser heat source is removed, the lattice temperature keep rising due to continuous energy flux from the electron system until the thermal balance between two systems is reached. The balanced temperature is about $420\,^oK$ at t=18ps. Figure 5 shows the electron temperature for J=2000×10$^{-12}J/\mu m^2$. The stronger laser heat source boots the maximum electron temperature to about $6500\,^oK$, shown in Figure 5. It also takes a longer time to balance the energy flux between electrons and lattice. The electron temperature is still much higher than the lattice temperature after 20ps.
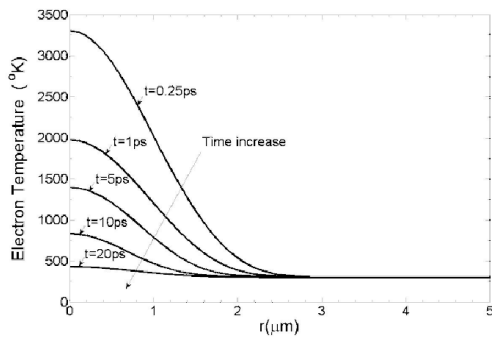
Figure 6 Electron temperature on the top in the r direction, (z=0) for J=500×10$^{-12}J/\mu m^2$.
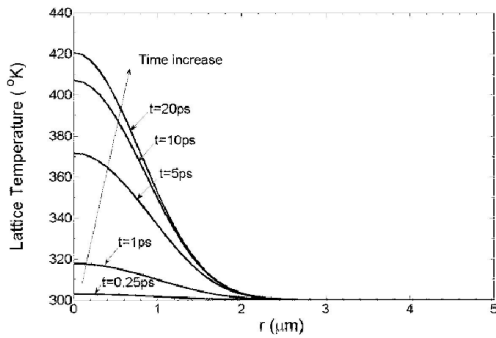
Figure 7 Lattice temperature on the top in the r direction, (z=0) for J=500×10$^{-12}J/\mu m^2$.

The electron and lattice temperatures along the r direction for t=0.25ps, 0.5ps, 1ps, 5ps, 10ps and 20ps are shown in Figure 6 and 7. The results show the coupling effects between the electron and lattice system. It is noted that the effects of the thermal wave is not significant in r direction since the length is much longer than the thickness. It is noted that there is no significant temperature change for r>2.5μm.

Figure 8 and 9 show the electron and lattice temperature along the z direction at different time increments. At t=0.25ps, there is a significant temperature difference, about 2750°K, between the top and bottom surface. The effects of thermal wave propagation are indicated by decrease of electron temperature on the top and increase at the bottom. The

temperature difference between the top and the bottom reduces to about 300°K at t=0.5ps. The electron temperature is almost uniformly distributed along the z-direction after t=1ps. This uniform temperature gradually reduces due to the electron/lattice coupling effects. Because the lattice has a larger heat capacity, the change of lattice temperature is not as dramatic as the electron, shown in Figure 9. The lattice temperature on the top increases first and on the bottom follows. It is mainly due to the difference between the electron and lattice temperature.

Figure 10 shows the lattice heat flux in the z direction on the centre axis. The major electric heat flux occurs within 0.5ps. After that, its magnitude drops quickly to the level of the lattice heat flux, which has the larger values in the middle region around t=0.5ps. Figure 11 to 14 show the temperature distribution of the electron and the lattice at several difference time increments.
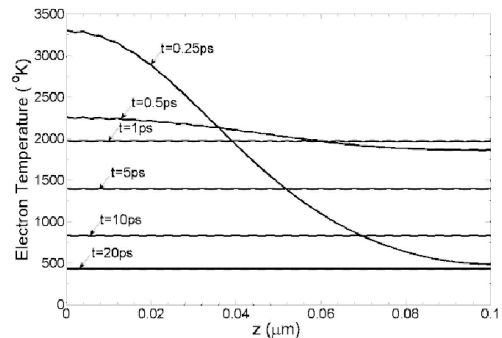

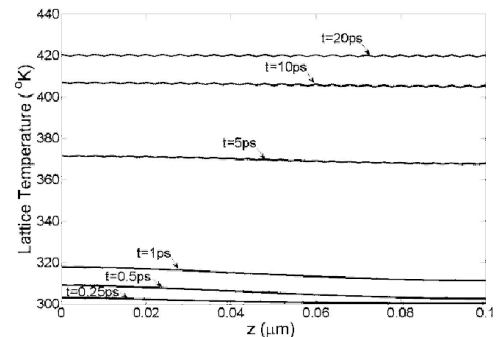**Figure 8** Electron temperatures along the centre axis

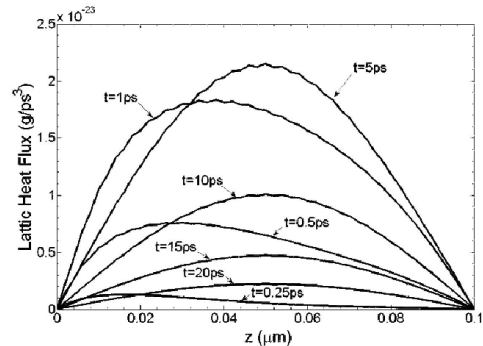**Figure 9** Lattice temperatures along the centre axis

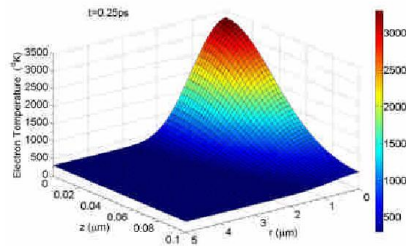**Figure 10** Lattice heat flux q^z along the centre axis

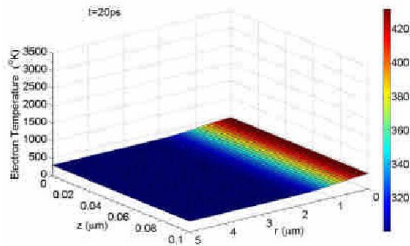**Figure 11** Electron temperature distribution at t=0.25*ps*

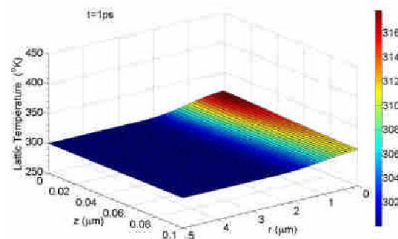**Figure 12** Electron temperature distribution at t=20*ps*

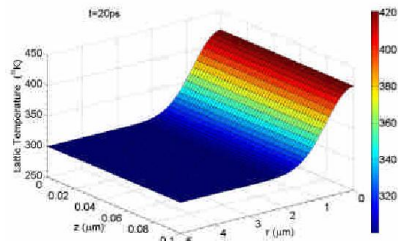**Figure 13** Lattice temperature distribution at t=0.5*ps*

Figure 14 Lattice temperature distribution at t=20*ps*

CONCLUSION

Temperature distribution for an axisymmetric heat transfer problem of a thin film exposed to an ultrashort-pulsed laser is successfully determined using the proposed hybrid differential transform/finite difference method. The maximum electron temperature can reach as high as several thousand degrees. The equilibrium electron/lattice temperature is only a couple hundred degrees. The results find obvious thermal wave propagation along the *z* direction. The recursive procedure can be implemented easily and efficiently.

REFERENCES

[1] Wang, H.J., Dai, W.Z., and Hewavitharana, L.G., A finite difference method for studying thermal deformation in a double-layered thin film with imperfect interfacial contact exposed to ultrashort pulsed lasers, *International Journal of Thermal Sciences* Vol. 47, 2008, pp.7–24

[2] Nolte, C.S., Chichkov, B.N., Alvensleben, F.V. and Tunnermann, A., Precise laser ablation with ultrashort pulses, *Appl. Surf. Sci.* Vol.109, 1997, pp.15–19.

[3] Shirk, M.D. and Molian, P.A., A review of ultrashort pulsed laser ablation of materials, *J. Laser Appl.* Vol.10, 1998, pp.18–28

[4] Anisimov, S. I., Kapeliovich, B. L. and Perel'man, T. L., Electron emission from metal surfaces exposed to ultra-short laser pulses, *Soviet Physics, JETP39*, 1974, pp.375-377.

[5] Qiu, T.Q. and Tien, C.L., Short-pulse laser heating on metals, *International Journal of Heat and Mass Transfer,* Vol. 35, 1992, pp.719-726.

[6] Qiu, T.Q. and Tien, C. L., Heat transfer mechanisms during short-pulse laser heating of metals, *Journal of Heat Transfer*, Vol.115, 1993, pp.835-841.

[7] Al-Nimr, M.A., Haddad, O.M. and Arpaci, V.S., Thermal behavior of metal films—A hyperbolic two-step model, *Heat Mass Transfer*, Vol. 35, 1999, pp.459–464.

[8] Chen, J.K. and Beraun, J.E., Numerical study of ultrashort laser pulse interactions with metal films, *Numer. Heat Transfer* A, Vol. 40, 2001, pp. 1–20.

[9] Al-Odat, M., Al-Nimr, M.A. and M. Hamdan, Thermal stability of superconductors under the effect of a two-dimensional hyperbolic heat conduction model, *Int. J.Numer. Meth. Heat Fluid Flow*, Vol. 12, 2002, pp.173–177.

[10] Naji, M., Al-Nimr, M.A. and M. Hader, The validity of using the microscopic hyperbolic heat conduction model under harmonic fluctuating boundary heating source, *Int. J. Thermophys.*, Vol. 24, 2003, pp.545–557.

[11] Jiang, L. and Tsai, H.L., Improved two-temperature model and its application in ultrashort laser heating of mental films, *Journal of Heat Transfer*, Vol. 127, 2005, pp.1167-1173.

[12] D.E. Glass, M.N. Ozisik, D.S. McRae, and B. Vick, On the Numerical Solution of Hyperbolic Heat Conduction, Numer. Heat Transfer, vol. 8, pp. 497–504, 1985.

[13] W. K. Yeung and T. T. Lam, A Numerical Scheme for Non-Fourier Heat Conduction, Part I: One-Dimensional Problem Formulation and Applications, Numer. Heat Transfer B, vol. 33, pp. 215–233, 1998.

[14] T. T. Lam and W. K. Yeung, A Numerical Scheme for Non-Fourier Heat Conduction, Part II: Two-Dimensional Problem Formulation and Verification, Numer. Heat Transfer B, vol. 41, pp. 543-564, 2002

[15] Chen, C.L. and Liu, Y.C., Solution of two-boundary-value-problems using the differential transform method, *Journal of Optimization Theory and Application*, 99, 1998, pp. 23-35.

[16] Yu, L.T. and Chen, C.K., The solution of the Blasius equation by the differential transform method, *Math. Comput. Modeling,* Vol. 28, No.1, 1998, pp. 101-111, 1998.

[17] Chen, J.K., Latham, W.P. and Beraun, J.E., Axisymmetric modeling of femtosecond-pulse laser heating on metal films, *Numerical Heat Transfer* B, Vol. 42, 2002, pp1-17.